Chamber Influence Estimation for Radiated Emission Testing in the Frequency Range of 1 GHz to 18 GHz

Alexander Kriz
Electromagnetic Compatibility and RF-Engineering
ARC Seibersdorf research GmbH
Seibersdorf, Austria
alexander.kriz@arcs.ac.at

Wolfgang Müllner
Electromagnetic Compatibility and RF-Engineering
ARC Seibersdorf research GmbH
Seibersdorf, Austria
wolfgang.muellner@arcs.ac.at

***Abstract*—The paper presents a comprehensive analysis of the behavior of anechoic chambers in the frequency range from 1 GHz to 18 GHz. Numerical simulation and statistical analysis have been used to estimate the influence of the test site to radiated emission results above 1 GHz. For typical EMC chambers the influence factor is around 0.7 dB. This factor can be improved by using better absorbing material or increasing of chamber size. For a wide range of EUT's the compliance uncertainty can be estimated using the chamber influence factor. The prediction of the chamber influence for small omnidirectional EUT's fits very well. Small EUT's with a directive disturbance source are overestimated. Large EUT's with multiple sources have not been investigated.**

Anechoic chamber; radiated emission testing; chamber validation; EMC above 1 GHz; compliance uncertainty

I. INTRODUCTION

The development of a standard to measure radiated emissions above 1 GHz is an important topic of the EMC community in the last years. CISPR is working toward this since 2002 with high pressure.

The definition of a new measurement technique is quite a complex task. In case of a radiated emission test procedure the project can be split into several independent problems. First of them is the development of the measurement method itself. For this method the calculation of the measurement uncertainty is required. Measurement uncertainty is also called compliance uncertainty, if the measurement is aimed to test the compliance of a EUT. To estimate the compliance uncertainty all factors which influence the result of the measurement have to be determined. The most important factors are the influence of the test site, the calibration uncertainty of the receive antenna, the uncertainty of the cable loss and the uncertainty of the test receiver. The procedure how to combine these factors to the compliance uncertainty has to be done according to the GUM [1] [2] or to CISPR 16-4-2 [3].

This paper proposes a method how to estimate the influence of the test site on the radiated emission test result.

II. SITE IMPERFECTIONS BELOW 1 GHZ

A. Basics of Validation

The basic idea of the validation technique is to substitute the EUT by a radiation source. The radiation pattern of each EUT is different and unknown, so the properties of a general EUT have to be assumed. These are omnidirectional radiation characteristic and no near field coupling with the test site. This general EUT is placed at the test site and the electrical field strength is measured. The result is compared to a pre-calibrated field strength and a maximum difference is allowed.

One possibility to realize such a EUT is to use broadband antennas like Bicones or Log Periodic Antennas, which are driven by a signal generator or a comb generator. This approach is realized by all test site validation standards like CISPR [4], ANSI [5], ETSI [6] and VCCI [7]. Of course there are some difficulties to keep in mind. The first one is the near field coupling of biconical antennas with the ground plane. This is solved by introducing a dual antenna factor [8]. Another problem is that Log Periodic Antennas are not omnidirectional. In new standards like CENELEC [9] the problem is avoided by using small biconical antennas up to 1 GHz.

B. Normalized Site Attenuation

In a paper from A. A. Smith [10] the use of a Normalized Site Attenuation (NSA) is suggested. This technique fits very well to the ideas presented above. The EUT is replaced by a calibrated antenna. The traceability of the NSA method is ensured by calibration of both antennas.

The limit of 4 dB NSA deviation used by ANSI and CISPR is calculated by adding the uncertainty contribution of 1 dB for each antenna, 1 dB for the receiver and 1 dB for the test site. A common mistake in the understanding of NSA testing is to think that a test site has a deviation of 4 dB. The site deviation is only 1 dB and the remaining 3 dB is the validation uncertainty. Of course this way of dealing with uncertainty is not state-of-the-art, but it is still applicable.

III. SITE IMPERFECTION ABOVE 1 GHZ

Due to physics there is a different situation above 1 GHz. Some of the before mentioned effects also occur here, some can be neglected, but there are also new effects.

The effect of the absorbers – electromagnetic wave is attenuated by the reflectivity – is nearly identical. The dependency of the reflectivity from the impinging angle becomes more important. How strong the impinging wave is scattered by the absorber depends on the absorber quality and shape.

The influence of near field coupling between the EUT and the environment can be neglected. The wavelength is small compared to the distance to the absorber, so the reactive near-field region is not disturbed by the surroundings.

A new effect is the strong directivity of the receive antenna. In this frequency range widely common antennas are double ridged horn antennas and log periodic antennas. Their gain is approximately 12 dBi for horn antennas and 7 dBi for log periodic antennas. This results in a lower sensitivity to the surroundings, because the antenna faces the EUT and reflected waves are not impinging the antenna in the main lobe.

IV. NUMERICAL SIMULATION

In this paper the influence of the anechoic chamber is calculated by numerical simulation.

A. Model of Anechoic Chambers

Before building up a model some assumptions have to be made, which are valid for the desired frequency range:

- The radiation characteristic of the EUT is strongly depending on the type of the equipment. There are test objects with strong main lobes possible as well as omnidirectional radiators. We assumed an omnidirectional characteristic, because this case will lead to the strongest influence of the anechoic chamber.
- The test site can be any reflection free environment. We choose a cubic anechoic chamber because most of the sites will be of that type.
- The receive antenna is a wide band horn antenna (double ridged horn antenna) with a narrow beam width and a good front to back ratio.
- The performance of the absorbing material is described by the reflectivity. Only reflected waves are taken under consideration, scattered waves are neglected.
- Only single reflections are taken into consideration, see Fig. 1. The energy of multiple reflections is to low to change the received field strength significantly when typical absorbers are used.

Physical effects are not considered like the near-field coupling (reactive near-field region). Another neglected effect is the dependency of the reflectivity to the impinging angle.

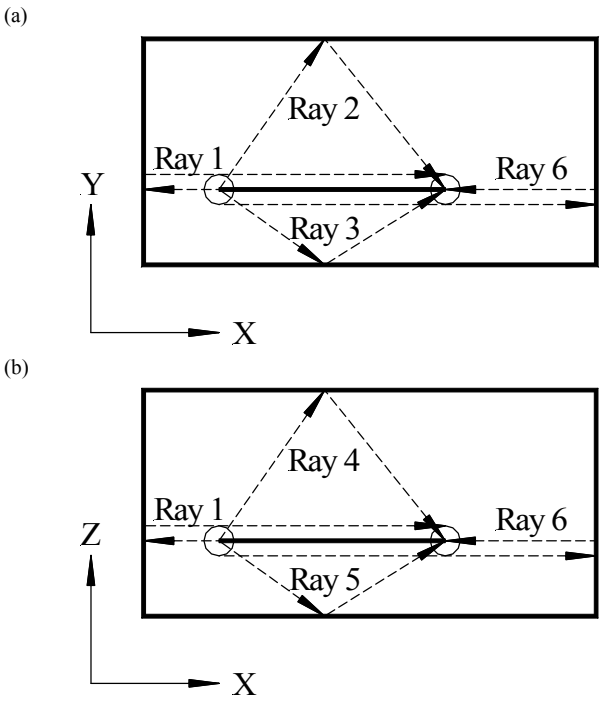

Figure 1. Considered reflected rays and their designation
(a) top view (b) front view

For each ray a complex wave equation for the received field strength is assumed [11]. See (1) for the Poynting vector of the direct ray E_D, where D is the distance between transmitter and receiver and λ is the wavelength.

$$\underline{\vec{S}}_D = e^{-j\frac{2\pi D}{\lambda}} \cdot \vec{e}_D \tag{1}$$

The impinging angle of the Poynting vector is determined by a unit vector.

$$\vec{e}_D = \vec{e}_X \tag{2}$$

There are six reflected rays assigned as Ray1 to Ray6. The free space attenuation for the different path length is taken under consideration by multiplying the ratio of the direct length D and the length of the current ray W_X. The pattern factor PF_X considers the radiation characteristics of the receive antenna. This factor attenuates the ray additional to the absorber reflectivity R.

$$\underline{\vec{S}}_{RayX} = 10^{\frac{-R+PF_X}{20}} \cdot \frac{D}{W_X} \cdot e^{-j\frac{2\pi W_X}{\lambda}} \cdot \vec{e}_{RayX} \tag{3}$$

The impinging angles of the Poynting vectors are determined by the unit vectors, e.g.

$$\vec{e}_{Ray1} = \vec{e}_X$$
$$\vec{e}_{Ray6} = -\vec{e}_X \quad (4)$$

The chamber influence I in dB is calculated according to (5). The Poynting vectors of all six reflected rays and the direct ray are added and related to the Poynting vector of the direct ray.

$$I = 20 \cdot \log \left| \frac{\underline{\vec{S}}_D + \sum_{X=1}^{6} \underline{\vec{S}}_{RayX}}{\underline{\vec{S}}_D} \right| \quad (5)$$

The directivity of a typical receive antenna is shown in Fig. 2. This antenna is double ridged horn antenna for the frequency range from 1 GHz to 18 GHz.

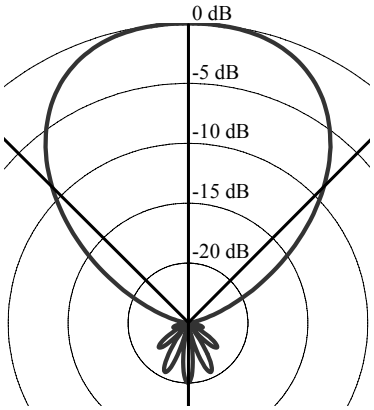

Figure 2. Radiation pattern of a typical receive antenna

From this figure the pattern factors PF_X for each ray can be read. The direct ray S_D and S_{Ray1} are impinging at angle 0°, so the pattern factors reads 0 dB. The reflected ray from the wall behind the receive antenna S_{Ray6} reads - 20 dB. The rays reflected from ground, ceiling and the side walls are impinging at an angle of approx. ± 45 °. The pattern factor in this case is around - 9 dB. Due to this behavior it becomes obvious that high gain antennas are less sensitive to the test site than low gain antennas.

TABLE I. PATTERN FACTORS PF_X

Angle [°]	Pattern Factor PF_X [dB]	Ray No.
0	0	1
≈ ± 45	≈ - 9	2, 3, 4, 5
180	- 20	6

B. Statistical Evaluation of Chamber Influence

All assumption made till now concern physics only and no specific properties of an anechoic chamber. Now we assume a typical compact fully anechoic chamber, with a size of 7 m (length) by 4 m (width) by 3.5 m (height). The test distance is 3 m and the absorber reflectivity 20 dB.

We scanned through a volume to estimate the chamber influence I, where the distance between transmit and receive antenna is kept constant, see Fig. 3. The size of the cube is 1 m by 1 m by 1 m and the bottom of the cube has a distance of 1 m to the floor of the anechoic chamber. Regarding to the X and Y axis the cube is located in the middle of the chamber. The observed frequency is 1 GHz, so the size of the plane is larger than the wavelength.

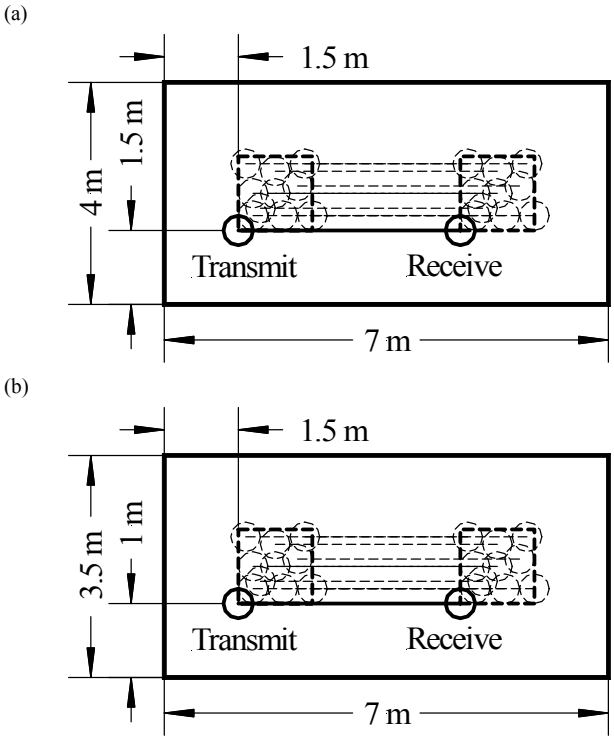

Figure 3. Scanning through a test volume (a) top view, (b) front view

The chamber influence I can be visualized in a 3D diagram, see Fig. 4, where we cut through the XY-plane at a height of 1.2 m. The result is a wave pattern and has about six sine periods in the X axis. This is approximately twice the wavelength, due to a wavelength of 30 cm and a plane length of 1 m. The reason for this is that the path difference is twice as high as the movement along the X axis. The reflected ray has to travel to the wall and back.

We can observe that the influence in the volume can be any value between - 1.0 dB and + 0.95 dB, dependent from the chosen point. Therefore we need to use a statistical analysis to calculate a probable influence factor. The interval of I is not symmetrical due to the non-linearity of the logarithm.

One can calculate the probability distribution - also called Distribution Function P (I), see Fig. 5. The diagram is normalized that the area below the curve corresponds to 100 %. The distribution is very similar to the Rice distribution. This distribution occurs also at mobile communication channels. In this application there is a similar situation – multiple signals arriving from different directions and with different signal levels and one dominant signal (line-of-sight).

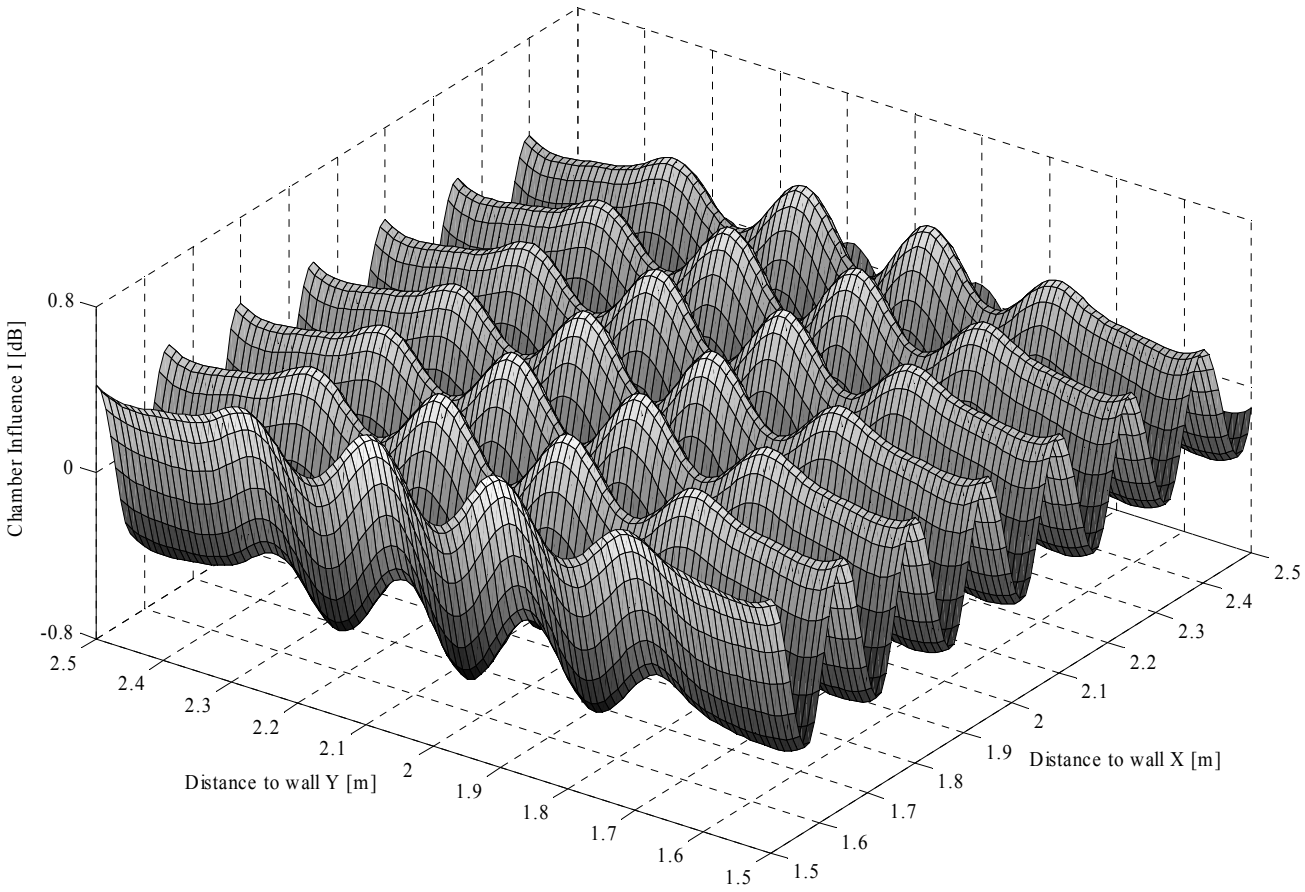

Figure 4. Chamber Influence I in XY-plane at a height of 1.2 m

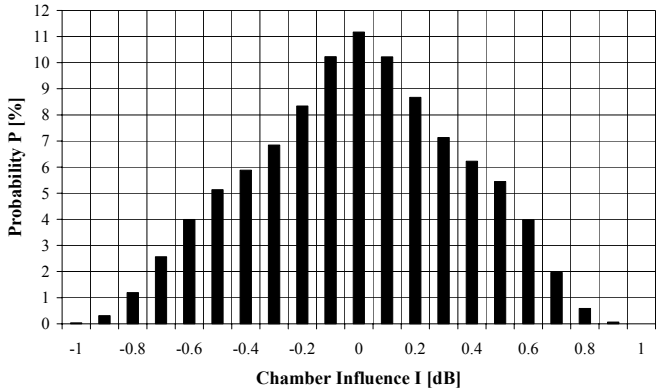

Figure 5. Distribution Function P(I)

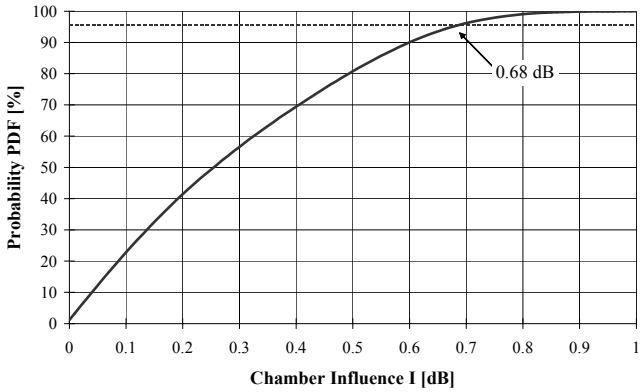

Figure 6. Probability Density Function PDF(I)

With the Distribution Function we know the probability that a certain test site influence occurs. More relevant is the probability that the chamber performance is better than a certain value, e.g. 1 dB. Therefore the Probability Density Function (PDF) is calculated by using the Distribution Function P:

$$PDF(I) = \int_0^I P(x) + P(-x)dx \qquad (4)$$

Using the PDF (I), Fig 6 can be read: "At 95 % of all points in the test plane the test site influence is less than ± 0.68 dB".

Common standards for calculation of the measurement uncertainty [1] [2] are using standard deviations with coverage factors of 95 %. So we define the probable chamber influence PCI at 95 %.

$$PCI = PDF(95\%) \qquad (5)$$

C. *Examples of chamber influence investigation*

To investigate the influence of the absorber reflectivity on the probable chamber influence, we kept the chamber size (7 m by 4 m by 3.5 m) constant and varied the reflectivity R from 5 dB to 40 dB.

This result of the simulation is compared to a very simple estimation by Hollis [12].

$$PCI = 20 \cdot \log\left(1 + 10^{-\frac{R}{20}}\right) \tag{6}$$

This calculation assumes a direct ray and one reflected ray in phase. The reflected ray is only attenuated by the reflectivity and not by the larger path length.

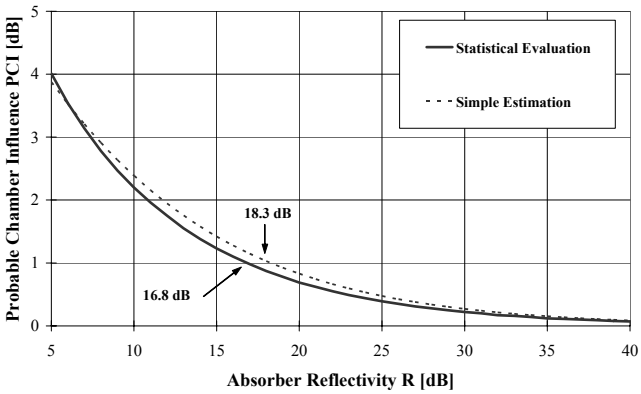

Figure 7. Influence of reflectivity to probable chamber influence

The results for the statistical evaluation and the simple estimation are shown in Fig. 7. Remarkable is the good correspondence, although the calculations are based on completely different assumptions.

The required reflectivity to get a probable chamber influence of 1 dB is 18.3 dB for the simple estimation. The complex simulation leads to value of 16.8 dB, so the difference is only 1.5 dB in the absorber reflectivity.

Another investigation is to calculate the influence of the chamber size. To do so we kept the absorber reflectivity constant (R = 20 dB) and changed the size of the chamber by a Size Factor.

The dimensions of the chamber (length, width and height) are multiplied by the Size Factor, see (5) and Fig. 8. The Size Factor is varied from 1 to 11. A Size factor of 11 leads to a huge chamber of 77 m by 44 m and 38.5 m. Of course such chambers have no practical relevance, but they can be compared to Open Area Test Sites, where only the ground setup influences the result.

$$\begin{aligned} Length' &= Length \cdot Size\ Factor \\ Width' &= Width \cdot Size\ Factor \\ Height' &= Height \cdot Size\ Factor \end{aligned} \tag{5}$$

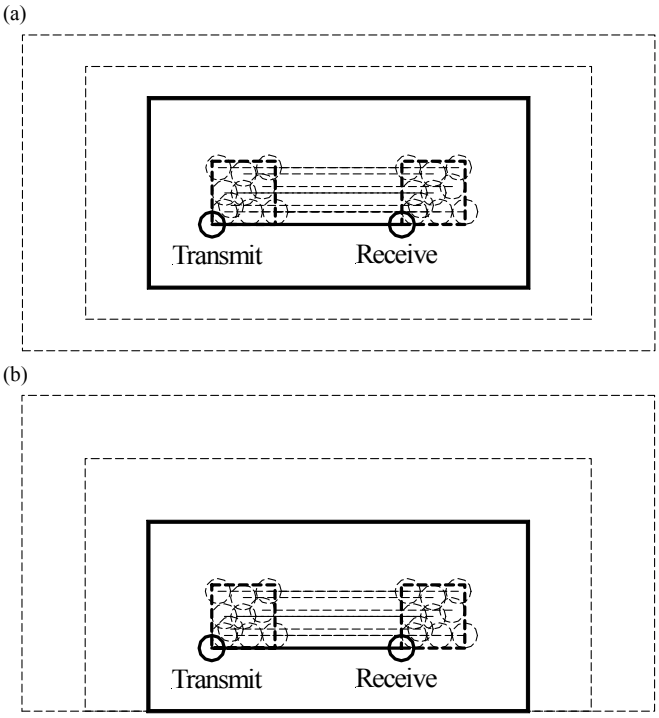

Figure 8. Changing the chamber size (a) top view, (b) front view

Even at very large Size Factors the PCI is not decreased to zero, see Fig. 9. The reason for this is the absorber layout at the ground, which influence is not decreased by changing the Size Factor.

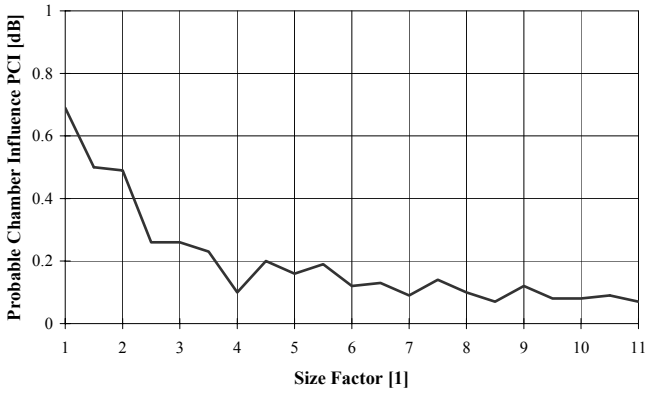

Figure 9. Probability density

Using Fig. 7 and Fig. 9 we can estimate how effective an improvement of chamber performance could be. If want to halve the probable chamber influence from 0.7 dB to 0.35 dB, we can increase the absorber reflectivity by 6 dB to 26 dB. The other possibility to reach this goal is to build a chamber which is 3.5 times larger.

V. MEASUREMENT OF THE TEST SITE INFLUENCE

The measurement of the test site influence is called chamber validation. This chamber validation is performed similar to the validation technique below 1 GHz.

An omnidirectional antenna is used as transmit antenna. This antenna is placed to defined locations in the test volume. The site attenuation is measured to a receive antenna, where the distance between the antennas are kept constant. The receive antenna should be the same antenna type like it is used for emission measurements and it is facing the transmit antenna. A calibration of both antennas is not necessary, because one has to look only to the spread of the site attenuation. This spread is called site VSWR. The determination of the NSA is not required.

It is very hard to build omnidirectional antennas up to 18 GHz. Commercial available are at the moment conical monopoles up to approx. 6 GHz and biconical antennas up to 3 GHz. Due to the lack of suitable antennas to 18 GHz, it is also possible to use a reciprocal technique. The omnidirectional transmit antenna is replaced by an isotropic field probe and the electric field is transmitted with the "receive" antenna. The disadvantage of this method is the need for power amplifiers up to 18 GHz.

VI. Estimation of Uncertainty Contribution

The PCI simulated in the previous chapters describes the influence of the anechoic chamber to the radiated emission test. The assumptions are an omnidirectional small EUT and a typical directive receive antenna. These assumptions lead to the strongest possible influence of the chamber to the radiated emission test result. A EUT with directive characteristic illuminates the chamber less and therefore the radiated emission result depends less on the chamber performance. Therefore the PCI can be used as uncertainty contribution in the calculation of the measurement uncertainty of omnidirectional equipment. Using the PCI for small directive EUT's is possible as no underestimation of the influence occurs.

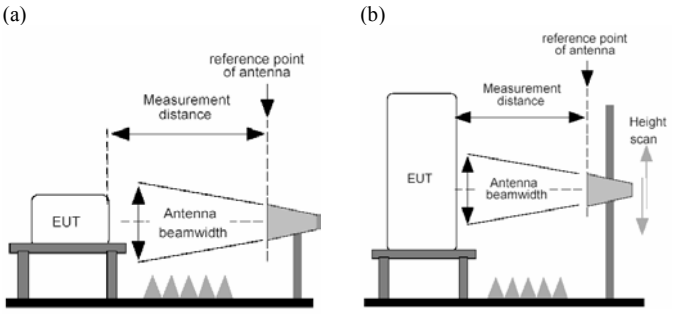

Figure 10. Emission measurement for (a) small and (b) large EUT's

Large EUT's may contain multiple radiation source and due to its size a height scan of the receive antenna is required, see Fig. 10. Further investigation needs to be performed to ensure the validity of the PCI.

VII. Conclusion

This paper presents a comprehensive analysis of the behavior of anechoic chambers in the frequency range from 1 GHz to 18 GHz. A simulation model is built to calculate the influence factor of a chamber. An omnidirectional source radiates a direct and six reflected rays. Absorber and receive antenna pattern data are considered in the calculation of the influence. By scanning through volumes and statistical analysis a probable influence factor PCI is estimated. We investigated the dependency from the absorber reflectivity and chamber size. The suggested PCI can be used for the radiated emission uncertainty for a wide range of EUT's.

References

[1] BIPM, IEC, IFCC, ISO, IUPAC, IUPAP, OIML: "Guide to the Expression of Uncertainty in Measurement (GUM)", 1993

[2] EA-02/04: "Expression of the Uncertainty of Measurement in Calibration", EA European co-operation for Accreditation, December 1999

[3] CISPR 16-4-2 - Ed. 1.0: "Specification for radio disturbance and immunity measuring apparatus and methods - Part 4-2: Uncertainties, statistics and limit modelling - Uncertainty in EMC measurements", November 2003

[4] CISPR 16-1-4 - Ed. 1.0: "Specification for radio disturbance and immunity measuring apparatus and methods - Part 1-4: Radio disturbance and immunity measuring apparatus - Ancillary equipment - Radiated disturbances", November 2003

[5] ANSI C63.4-2001: „American National Standard for Methods of Measurement of Radio Noise Emissions from Low-Voltage Electrical and Electronic Equipment in the Range of 9 kHz to 40 GHz", New York: IEEE, 2001

[6] ETSI ETR 273-2: "Electromagnetic compatibility and Radio spectrum Matters (ERM); Improvement of radiated methods of measurement (using test sites) and evaluation of corresponding measurement uncertainties; Part2: Anechoic chambers", European Telecommunications Standards Institute, February 1998

[7] VCCI: Regulations for voluntary control measures. 14th Edition, April 2000

[8] W. Müllner, H. Garn: "From NSA to site-reference method for EMC test site validation", Int. Sym. on EMC, Montreal 2001, page 948-953 vol. 2

[9] Technical Report EN50147-3:2001: "Electromagnetic Compatibility Basic Emission Standard Part 3: Emission measurements in Fully Anechoic Rooms", CENELEC, 2001

[10] A. A. Smith, R. F. German, J. B. Pate: "Calculation of Site Attenuation from Antenna Factors", IEEE Transaction on Electromagnetic Compatibility, Vol. EMC-24, No. 3, August 1982

[11] W. L. Stutzman, G. A. Thiele: „Antenna Theory and Design", Second Edition, John Wiley & Sons, Inc., 1998

[12] J. S. Hollis, T. J. Lyon, L. Clyton: „Microwave Antenna Measurements", Scientific-Atlanta Inc., 1970